Acta Crystallographica Section A
Foundations of Crystallography
ISSN 0108-7673

Received 25 November 2002
Accepted 24 January 2003

Structures of a hollow filamentary conical helix

Fang-Fang Xu* and Yoshio Bando

Advanced Beam Analysis Station, National Institute for Materials Science, 1-1 Namiki, Tsukuba, Ibaraki 305-0044, Japan. Correspondence e-mail: xu.fangfang@nims.go.jp

A hollow conical helix (HCH) of graphitic materials broadens the conical configuration by introduction of wrapping about 120° symmetry positions in addition to the traditional rotation about 60° symmetry sites. Complete structural models are established for a HCH and examined taking into account the rotation mode, coincidence site lattice (CSL), disclination angle and packing pattern. Combined with experimental observations, it is revealed that the size of the CSL, hence the density of the coincidence lattice sites, dominates the overlap configuration of a conical helix.

1. Introduction

Filamentary growth of graphite may have structures displaying curved basal sheets arranged in the form of cone-helices. Basal cones stack on top of one another, but interconnect in a helical fashion by a single screw dislocation along the axis of the conical fiber. The cones have been found to have well defined apex angles and hence disclination angles, which were ascribed to high densities of coincidence lattice sites (CLS) between overlapping layers (Double & Hellawell, 1974; Amelinckx *et al.*, 1992; Krishnan *et al.*, 1997). In general, disclination angles that lead to coincidence configuration include multiples of 60° and their combination with additional overlap angles (θ_{over}) of *e.g.* 13.2, 21.8 and 27.8°. The apex angle (α) for a cone is determined by the disclination angle (θ_D) as described by Double & Hellawell (1974):

$$\sin\alpha/2 = (2\pi - \theta_D)/2\pi.$$

So far, the wrapping performance in the formation of conical helices of graphite has exclusively been examined from the viewpoint of rotation about the 60° symmetry positions, *i.e.* the center of a hexagon in the honeycomb array. This is attributed to the consideration of the creation of stable defects like two- to five-membered rings during the nucleation of cones (Amelinckx *et al.*, 1992; Bourgeois, Bando, Kurashima & Sato, 2000). Rotation about the 120° symmetry positions, *i.e.* individual atoms in the filamentary sheet, will give rise to single-bridged atoms at the conical tips, which are apparently energetically unfavorable and cannot be the nuclei from which cones form. However, recently we observed HCH of graphitic boron nitride (BN) where the tips were removed out of each basal cone fragment, giving rise to continuous interior tunnels and the geometry of an Archimedes spiral (Xu *et al.*, 2003), as shown in Fig. 1. Transmission-electron-microscopy (TEM) observation found that all the nanotubes show an open cap. Then nucleation of HCH must be different from that of conical fibers and the ring-stacking model does not seem to be able to account for it. By being released from the requirement for forming stable defects at the initial growth stage, HCH broadens the conical configurations, some of which were

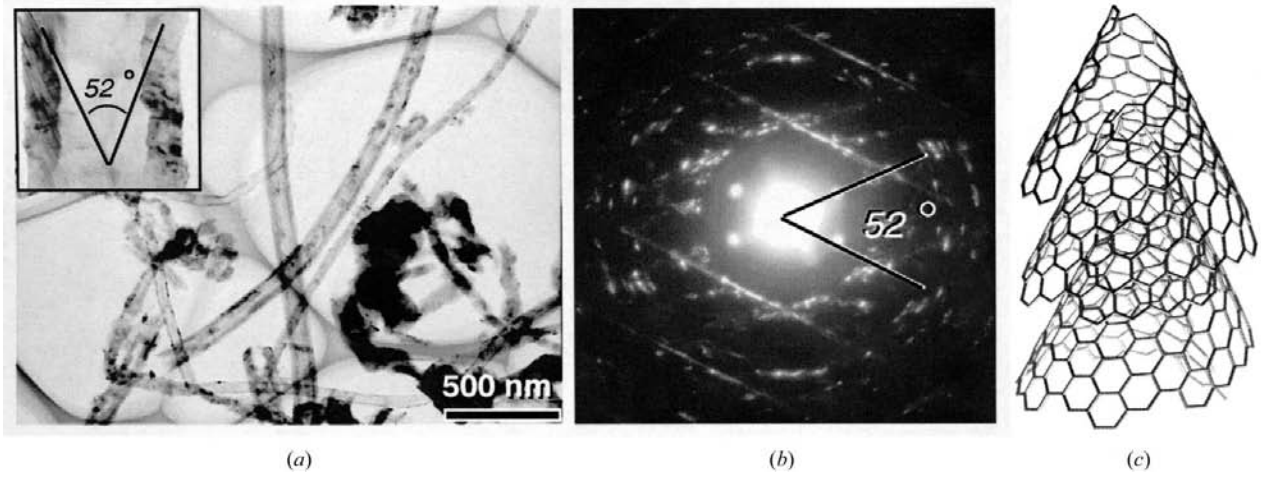

Figure 1
(*a*) TEM image and (*b*) typical diffraction pattern of the BN HCH. (*c*) Structural model of a hollow conical helix.

Table 1
Disclination configuration and CSL structures.

Disclination angles	CSL type and lattice parameter ($\times a_0$)†		CSL stacking patterns				
$(2k+1)\cdot 60^\circ$	Sixfold Threefold	BN-type Graphite type	$AA'AA'$ $ABAB$				
	1		About sixfold axis			About threefold axis	
$2k\cdot 60^\circ$	– 1		$AAAA$			$AAAA$	
$n\cdot 60\pm 21.8^\circ$	$\Sigma 7$ $\sqrt{7}$		ch∧ch			at∧at	$AAAA$
$n\cdot 60\pm 13.2^\circ$	$\Sigma 19$ $\sqrt{19}$		at∧at	$AA'AA'$	$n=2k$	at∧ch	$n=2k$
$n\cdot 60\pm 9.4^\circ$	$\Sigma 37$ $\sqrt{37}$		at∧at	$AAAA$	$n=2k+1$	ch∧ch	$n=2k+1$
$n\cdot 60\pm 27.8^\circ$	$\Sigma 13$ $\sqrt{13}$		ch∧ch			at∧at	$AAAA$
$n\cdot 60\pm 17.9^\circ$	$\Sigma 31$ $\sqrt{31}$		at∧at	$AA'AA'$	$n=2k+1$	at∧ch	$n=2k+1$
$n\cdot 60\pm 15.2^\circ$	$\Sigma 43$ $\sqrt{43}$		at∧at	$AAAA$	$n=2k$	ch∧ch	$n=2k$

† a_0 represents the basic in-plane lattice parameter of graphitic structure.

previously considered impossible. Rotation about a 120° symmetry position should be taken into account. Here, theoretical modeling and examination of HCH structures are reported.

2. Experimental details

BN HCH was obtained by employing a synthesis kinetics similar to that previously reported, which prepared conventional BN nanotubes *via* a substitution reaction from C nanotubes (CNTs) by B_2O_3 in N_2 atmosphere (Han *et al.*, 1998). However, a post-heating process at an increased temperature is undertaken in the present synthesis. Details of synthesis and formation mechanism of BN HCH have been described elsewhere (Xu *et al.*, 2003). TEM observations (Fig. 1*a*) on a field-emission JEOL 3000 F analytical microscope operated at 300 kV revealed large quantities of nano-sized tubules, displaying oblique filaments (inset of Fig. 1*a*) relative to the tube axis. This, along with the electron diffractometry (Fig. 1*b*), which is in good agreement with the reported conical structure (Bourgeois *et al.*, 1999), indicates a geometry characteristic of hollow conical helices (Fig. 1*c*). X-ray diffractometry (XRD, Cu $K\alpha$) and chemical analysis by electron energy-loss spectroscopy (EELS, Gatan DigiPEELS 766) suggested a pure graphite-like BN phase with lattice parameters a = 2.502 and c = 3.333 Å. Experimental work found that the apex angles of HCH depended on the synthesis temperatures. Higher temperature has given rise to larger apex angles and small tubular radius. Moreover, a quite narrow distribution of apex angles was revealed for each specimen prepared at different temperatures, for example, BN HCH synthesized at 2073 K displays a distribution of apex angles in the range 43.4–60°, which peak at 52° (Figs. 1*a*,*b*), hence a peaked disclination angle at 180 + 21.8°. It seems that the thermal dynamic element (enthalpy) alone determines the disclination angles and tubular radius of HCH. However, only three θ_{over} have been observed in the present materials synthesized between 2023 and 2073 K, they are 21.8, 27.8 and 13.2°.

3. Structural analysis

For a graphitic filamentary structure, the CSLs that guarantee the wrapping configurations are obtained only when rotation is performed about either 60° (sixfold) or 120° (threefold) symmetry positions. Rotation about sixfold symmetry positions has been widely studied for both graphite and BN systems (Double & Hellawell, 1974; Amelinckx *et al.*, 1992, 1996; Krishnan *et al.*, 1997; Bourgeois *et al.*, 1999; Bourgeois, Bando, Han & Sato, 2000; Bourgeois, Bando, Kurashima & Sato, 2000). Here, a statistical examination of rotation about both sixfold and threefold symmetry positions is presented and comparison is made with respect to the lattice parameters and stacking configuration of CSLs and disclination angles. Fig. 2 describes CLSs displaying different CSL parameters and hence different disclination angles. CLSs for a certain CSL or disclination angle lie on a circle about the rotation axis (*i.e.* either the center of a hexagon or an individual atom). The radius of the circle equals the lattice parameter of the CSL. The angle between two neighboring CLSs on a certain circle refers to θ_{over} included in the disclination configuration. In the sixfold scheme (where rotation is performed about the sixfold symmetry positions), the CLSs on a certain circle have the same type, *i.e.* either all atoms or all hexagonal centers. However, different types of CLS may occur on a circle in the threefold scheme (where rotation is performed about the threefold symmetry positions). Therefore, for the rotation about a sixfold axis, CLSs only display atom-on-atom (at∧at) and channel-on-channel (ch∧ch) packing while an additional atom-on-channel (at∧ch) CLS is available after rotation about a threefold axis. The shaded regions in the sixfold scheme and the lines in the threefold scheme pass through the CLSs for $n\cdot 60^\circ$ disclination. Configurations involving $\theta_D = n\cdot 60^\circ$about a sixfold axis should be preferred since each turn of the helix could bring successive layers back into exact coincidence. The lattice parameter for such CSLs equals the basic in-plane unit of the graphitic structure. Anyhow, the packing between the successive filaments is found to employ different sequences depending on the n value. The h-BN-type $AA'AA'$ stacking is available when $n = 2k + 1$, *i.e.* for disclination angles of 60, 180 and 300°, whereas the $AAAA$ stacking sequence occurs when $n = 2k$, *i.e.* for 120 and 240° disclination. In graphite, there is no difference between these two types of stacking since only a unique element carbon is involved in the construction. $AA'AA'$ and $AAAA$ are actually the same and energetically unfavorable. However, for a binary system like graphitic BN,

A/A' represents the stacking of B atoms onto N atoms and *vice versa* while A/A refers to the packing of the same element over itself. $AA'AA'$ stacking is apparently much more favorable than the $AAAA$ sequence for the BN system. It should be noted that the disclination-dependent configuration for a BN conical helix is different from that for a non-helical cone structure, where packing of monolayered BN cones shows preferred disclination angles of 120 and 240°, whereas the $(2k + 1) \cdot 60°$ disclination will introduce a row of B—B or N—N bonds at the connection, and hence be unfavorable (Bourgeois, Bando, Han & Sato, 2000).

As clearly seen in the threefold scheme, where a circle can cut simultaneously the atoms and the centers of channels, it is then possible that atoms coincide with the positions of channels after rotation of $n \cdot 60°$, giving rise to the $ABAB$ stacking sequence, *i.e.* the exact graphite type. Such a configuration cannot be obtained in the sixfold scheme. Similarly, there is also a rule to classify the stacking configuration of CSLs. $ABAB$ stacking appears only when $\theta_D = (2k + 1) \cdot 60°$ while $\theta_D = 2k \cdot 60°$ leads to the unfavorable $AAAA$ sequence. The CSL configurations for both sixfold and threefold cases are summarized in Table 1 and the structural models for $\theta_D = 180°$ are illustrated in Fig. 3 for the two wrapping modes.

When an additional θ_{over} is combined with the $n \cdot 60°$ disclination, the former configuration does not apply any longer and the CSLs may show various sizes and packing patterns. Among those additional overlap angles, the smallest CSL is found to form when $\theta_{over} = 21.8°$. Table 1 lists the six smallest CSLs and their disclination angles. The circles for $\theta_{over} = 21.8°$ and $\theta_{over} = 27.8°$, *i.e.* the two smallest CSLs, are illustrated in Fig. 2. They show CSL parameters of $\sqrt{7}$ and $\sqrt{13}$, and hence are denoted as $\Sigma 7$ and $\Sigma 13$ CSL, respectively. These two overlap angles have been frequently observed in graphitic conical helices. CSLs with larger lattice parameters have also been observed experimentally though not very often (Double & Hellawell, 1974; Amelinckx *et al.*, 1992; Krishnan *et al.*, 1997). Some CLSs for $\Sigma 19$ and $\Sigma 31$ CSLs are indicated in Fig. 2 by crosses and squares, respectively. The CSL structure is determined by the rotation mode (about threefold or sixfold axes), n value and θ_{over}, as summarized in Table 1. In case of rotation about a sixfold axis, CLSs could only be at∧at and ch∧ch, whereas they may be either at∧at and ch∧ch or at∧at and at∧ch for the rotation about a threefold axis. However, the at∧at coincidence sites show different packing sequences for the two rotation modes. Rotation about a threefold axis has exclusively $AAAA$ stacking while both $AAAA$ and $AA'AA'$ sequences may appear in CSLs when rotating about a sixfold axis. Figs. 4(*a*) and (*b*) show the $\Sigma 7$ CSLs with disclination of 120−21.8° for rotation about the sixfold and threefold axis, respectively, and Fig. 4(*c*) shows the $\Sigma 13$ CSL with disclination of 120−27.8°.

Our experimental observation found different apex angles depending on the synthesis temperatures (Xu *et al.*,

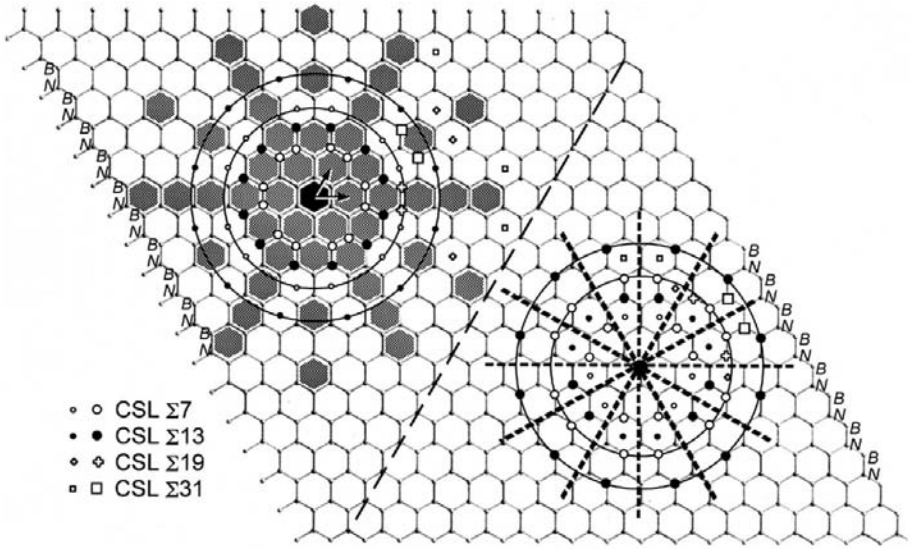

Figure 2
Distribution of coincidence lattice sites on a filamentary sheet for disclination about both a 60° symmetry position (left) and a 120° symmetry position (right).

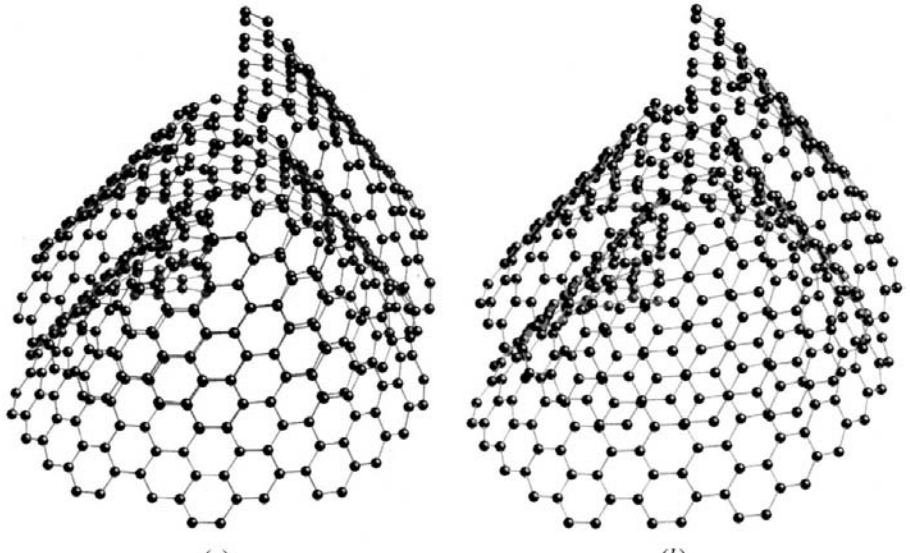

Figure 3
CSL structures of $\theta_D = 180°$. (*a*) is formed *via* wrapping about a 60° symmetry position and (*b*) about a 120° symmetry position.

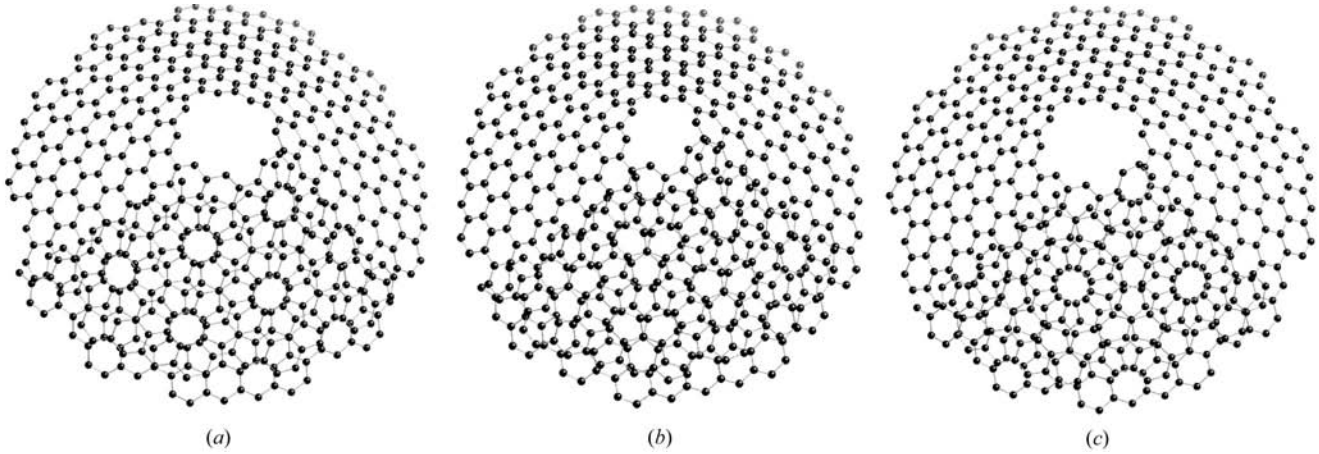

Figure 4
Different Σ7 CSL structures with disclination of 120−21.8°, which depend on wrapping about (*a*) a 60° symmetry position or (*b*) a 120° symmetry position. (*c*) is the Σ13 CSL structure with disclination of 120−27.8°, wrapping about a 60° symmetry site.

2003). The specimen heated at 2073 K shows a narrow distribution of apex angles which peak at ~52°, hence the disclination angle of 180 + 21.8°. However, the specimen heated at a lower temperature, *e.g.* 2023 K, exhibits a slight variety of apex angles, most of which are smaller than 52°. It can be seen from Table 1 that the disclination angle of 180 + 21.8° leads to the CSL configuration displaying CLSs of ch∧ch and *AAAA*-type at∧at irrespective of the rotation mode. The fact that a more stable configuration like the $AA'AA'$ type at∧at for the 180 + 27.8° disclination, which is close to the 180 + 21.8° disclination, is not employed implies that the size of the CSL, hence the density of CLSs, is the dominant factor determining the configuration of a conical helix rather than the stacking sequences. This is different from the BN graphitic plates, which prefer $AA'AA'$ to *AAAA* packing. In HCH, the highly curved filaments could only be stabilized *via* interlayer van der Waals forces, which are determined by both CSL and the packing pattern, *i.e.* the density of interlayer interaction and the type of interactions. It seems that high density of B—B and/or N—N type interactions gives rise to stronger interlayer bonding than low density of B—N type interaction. Anyhow, the synthesis temperatures determine the size and the apex angle (and hence the bending curvature and CSLs) of the final conical helices (Xu *et al.*, 2003).

4. Conclusions

Complete structural models for hollow conical helices are established in the present study. Wrapping of a graphitic filament about threefold symmetry positions, which has not been treated before, is examined and compared to the performance about traditional sixfold axes, taking into account the wrapping modes, CSLs, disclination angles and packing patterns. It has been found that the size of the CSL, hence the density of CLSs, is the dominant factor determining the conical configurations.

The authors wish to acknowledge Dr D. Golberg and Dr M. Mitome for the helpful discussion, and Dr R. Z. Ma, Dr Y. B. Li and Mr K. Kurashima for the assistance in experimental work.

References

Amelinckx, S., Devouard, B. & Baronnet, A. (1996). *Acta Cryst.* A**52**, 850–878.
Amelinckx, S., Luyten, W., Krekels, T., Van Tendeloo, G. & Van Landuyt, J. (1992). *J. Cryst. Growth*, **121**, 543–558.
Bourgeois, L., Bando, Y., Han, W. Q. & Sato, T. (2000). *Phys. Rev. B*, **61**, 7686–7691.
Bourgeois, L., Bando, Y., Kurashima, K. & Sato, T. (2000). *Philos. Mag. A*, **80**, 129–142.
Bourgeois, L., Bando, Y., Shinozaki, S., Kurashima, K. & Sato, T. (1999). *Acta Cryst.* A**55**, 168–177.
Double, D. D. & Hellawell, A. (1974). *Acta Metall.* **22**, 481–487.
Han, W. Q., Bando, Y., Kurashima, K. & Sato, T. (1998). *Appl. Phys. Lett.* **73**, 3085–3087.
Krishnan, A., Dujardin, E., Treacy, M. M. J., Hugdahl, J., Lynum, S. & Ebbesen, T. W. (1997). *Nature (London)*, **388**, 451–454.
Xu, F. F., Bando, Y., Ma, R. Z. & Golberg, D. (2003). *J. Am. Chem. Soc.* Submitted.